



Remediation of a soil chronically contaminated with hydrocarbons through persulfate oxidation and bioremediation



Rocío Medina^{a,b}, Pedro Maximiliano David Gara^c, Antonio José Fernández-González^{d,e}, Janina Alejandra Rosso^b, María Teresa Del Panno^{a,*}

^a Centro de Investigación y Desarrollo en Fermentaciones Industriales (CINDEFI), UNLP – CONICET, Calle 50 y 115, 1900 La Plata, Argentina

^b Instituto de Investigaciones Físicoquímicas Teóricas y Aplicadas (INIFTA), UNLP- CONICET, Diagonal 113 y 64, 1900 La Plata, Argentina

^c Centro de Investigaciones Ópticas (CIOp), CONICET – CIC - UNLP, Camino Parque Centenario e/55 y 508 Gonnet, C. C. 3 (1897), Gonnet, Argentina

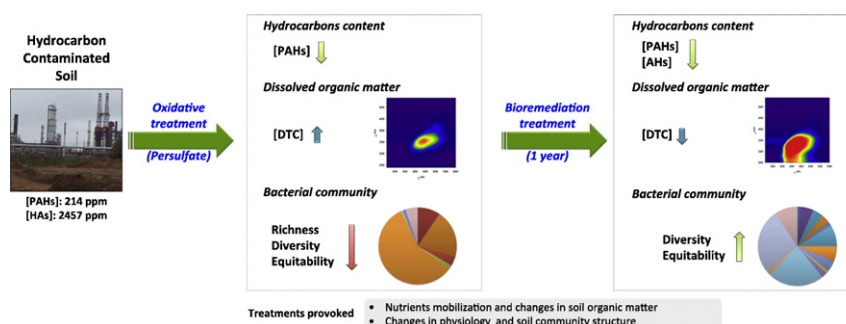
^d Université de Lorraine, Interactions Arbres–Microorganismes, UMR1136, F-54500 Vandoeuvre-lès-Nancy, France

^e INRA, Interactions Arbres–Microorganismes, UMR1136, F-54280 Champenoux, France

HIGHLIGHTS

- Effect of remediation chemical oxidation coupled biological treatment was evaluated.
- Spectroscopic analysis evidenced the oxidative changes on soil organic matter (SOM).
- SOM oxidation promoted the development of the resilient microbial community.
- The combined treatment increased the PAHs and aliphatic hydrocarbons elimination.

GRAPHICAL ABSTRACT



ARTICLE INFO

Article history:

Received 24 June 2017

Received in revised form 19 October 2017

Accepted 31 October 2017

Available online xxx

Editor: D. Barcelo

Keywords:

Chronically hydrocarbon-contaminated soil

Bioremediation

Chemical remediation

Coupled treatment for soil remediation

ABSTRACT

The impact of remediation combining chemical oxidation followed by biological treatment on soil matrix and microbial community was studied, of a chronically hydrocarbon contaminated soil sourced from a landfarming treatment. Oxidation by ammonium persulfate produced a significant elimination of polycyclic aromatic hydrocarbons (PAHs) and an increase in PAH bioavailability. Organic-matter oxidation mobilized nutrients from the soil matrix. The bacterial populations were affected negatively, with a marked diminution in the diversity indices. In this combined treatment with oxidation and bioremediation working in tandem, the aliphatic-hydrocarbon fractions were largely eliminated along with additional PAHs. The chemical and spectroscopic analyses indicated a change in soil nutrients. In spite of the high residual-sulfate concentration, a rapid recovery of the cultivable bacterial population and the establishment of a diverse and equitable microbial community were obtained. Pyrosequencing analysis demonstrated a marked succession throughout this twofold intervention in accordance with the chemical and biologic shifts observed. These remediation steps produced different effects on the soil physiology. Spectroscopic analysis became a useful tool for following and comparing those treatments, which involved acute changes in a matrix of such chronically hydrocarbon-contaminated soil. The combined treatment increased the elimination efficiency of both the aliphatic hydrocarbons and the PAHs at the expense of the mobilized organic matter, thus sustaining the

* Corresponding author at: Calle 50 y 115 número 227, 1900 La Plata, Argentina.

E-mail addresses: pedrogd@ciop.unlp.edu.ar (P.M. David Gara), antonio.fernandez-gonzalez@univ-lorraine.fr (A.J. Fernández-González), janina@inifta.unlp.edu.ar (J.A. Rosso), tere@biol.unlp.edu.ar (M.T. Del Panno).

recovery of the resilient populations throughout the treatment. The high-throughput–DNA-sequencing techniques enabled the identification of the predominant populations that were associated with the changes observed during the treatments.

© 2017 Elsevier B.V. All rights reserved.

1. Introduction

Intensive petrochemical activities have for years led to an increase in the contamination of soils around industrial facilities (Lemaire et al., 2013a). Indeed, such accumulated petrochemical sludge has continually needed the application of remediation treatments. According to the residual-hydrocarbon levels present, the material to be remediated can usually be handled within the petrochemical area. After an aging period, the residual contaminant nevertheless can persist in the soil or remediated material depending on the pollutant's availability, mobility, degradability, and/or reactivity (Huesemann et al., 2004; Stokes et al., 2006; Oleszczuk, 2007; Sutton et al., 2013; Tsibart and Gennadiev, 2013; Abdel-Shafy and Mansour, 2015).

Former petrochemical plant sites that were originally located on the outskirts of residential and business areas have now often become situated well within the limits of a city that has since developed. As a result, these contaminated sites are in close proximity to residential and commercial properties, municipal utilities, and roadway infrastructure. Consequently, the hazardousness of these areas needs to be evaluated and remediation interventions proposed.

Polycyclic aromatic hydrocarbons (PAHs) are pollutants of major concern because of their significant ecotoxicity, carcinogenicity, mutagenicity, and general toxicity to humans (Gupta et al., 2015; Ranc et al., 2016; Szczepaniak et al., 2016). The principal occurrence of PAHs in the environment is associated with anthropic activities such as petroleum and gas manufacturing and coke production (Bamforth and Singleton, 2005; Rivas, 2006; Gan et al., 2009). PAHs are strongly hydrophobic and thus poorly water-soluble, resulting in a long-term sequestration in various organic domains of the soil matrix (Sun et al., 2014).

In general, bioremediation has demonstrated success in eliminating PAHs from contaminated soil (Viñas et al., 2005; Asquith et al., 2012). The background information on the soil that has been studied, however, has suggested that bioremediation becomes inefficient in lowering long-term soil-hydrocarbon concentrations below the stringent environmental–clean-up standards, leaving frequently more or less complex residues (Plaza et al., 2009). Therefore, such situations require a more aggressive intervention.

Chemical oxidation is a promising technology that could overcome the current limitations on bioremediation. Different types of oxidants have been investigated for the remediation of contaminated soil including hydrogen peroxide, Fenton's reagent, persulfate peroxymonosulfate, permanganate, and ozone (Osgerby, 2006; Lim et al., 2016). Persulfate is increasingly being used for in-situ chemical oxidation (ISCO) of PAH-contaminated soils and groundwater (Liu et al., 2014; Peluffo et al., 2015). Stable at room temperature, persulfate can be activated via heat, transition metals, ultraviolet light, or other means to form the highly reactive sulfate radical, $\text{SO}_4^{\bullet-}$ (Tsitonaki et al., 2010; Matzek and Carter, 2016). Persulfate has been demonstrated to have a lower affinity for natural soil organics compared to other oxidants, therefore resulting in a higher remediation efficiency (Usman et al., 2012; Lim et al., 2016). Coupling chemical oxidation and bioremediation has produced successful results indicating improved remediation efficiencies compared with either the in-situ chemical oxidation or the bioremediation alone (Kulik et al., 2006; Valderrama et al., 2009; Mora et al., 2014). Nevertheless, the coupling of the two strategies could be complicated because of the effects on the autochthonous microbial community owing to the nature and degree of oxidation. Sutton et al. (2014a) attributed the absence of biodegradation to the high persulfate concentration originally applied in the

soil (about 10% in a slurry system) that did not allow the bacterial population to recover. Richardson et al. (2011), applying about a quarter of that persulfate concentration (2.7%) to a phenanthrene-contaminated soil in a column experiment, observed the recovery of the overall microbial community and, more significantly, recorded the presence of specific PAH-degrading bacterial groups during the bioremediation following persulfate treatment.

Few studies using persulfate oxidation under nonsaturating conditions have been carried out on contaminated soil. Mora et al. (2014) evaluated the feasibility of using a surface application of persulfate, thus maintaining the natural moisture content of a phenanthrene-contaminated soil. The authors evidenced an elimination of phenanthrene upon applying a low persulfate concentration ($<10 \text{ g} \cdot \text{kg}^{-1}$ dry soil) after 2 weeks; without any negative effects on the physicochemical and biologic properties of the soil.

The soil organic matter (SOM) exerts a strong influence on the efficiency of remediation treatments, not only because that parameter is related to the availability of the contaminants—which latter component is limited by both soil sorption and sequestration (Jonsson et al., 2007)—but also because an oxidant could interact with the SOM and the reduced inorganic compounds. The solubilized compounds upon partial oxidation could be assimilated by the resistant and/or conditioned microbial populations during the following bioremediation, thus enabling the recovery of that key biota. The oxidized molecules could also, however, shorten the persistence of the oxidant and scavenge the radicals produced (Rivas, 2006; Deng et al., 2015). Sutton et al. (2014a) observed the influence of the particular soil type on a coupled chemical and bioremediation treatment with different oxidants and emphasized the relevance of an adequate soil characterization to the efficiency of given remediation.

Excitation–emission matrix spectroscopy has become ever more frequently utilized for probing the composition, concentration, and dynamics of fluorescent organic matter from various source materials such as water, soil, and vegetables (Coble, 1996; Hudson et al., 2007; Cory et al., 2010; D'Andrilli et al., 2013; Andrade-Eiroa et al., 2013). PAHs and humic substances possess intrinsic fluorescence properties in the ultraviolet and blue spectral regions because of the constituent aromatic compounds (Dabestani and Ivanov, 1999). Hence, the study of excitation–emission spectroscopy of matrices constitutes a relevant modality for monitoring such contaminants and the nature of the organic matter simultaneously as a result of the molecular interactions between PAHs and the SOM (Fang et al., 1998; Akkanen et al., 2012; Ferretto et al., 2014).

Given the crucial necessity to maintain soil functions, considerable effort has been invested in the attempt to understand the response of soil ecosystems to environmental changes and the resistance and resilience of soil microorganisms (Griffiths and Philippot, 2013). Methods based on the polymerase-chain reaction (PCR) are strong investigative tools that do not depend on the growth of target organisms. Sutton et al. (2014a), analyzing the fingerprinting of the 16S-rRNA gene fragment by denaturing gradient gel electrophoresis (DGGE) and by band sequencing, observed differences in the microbial-community composition and diversity between different oxidative treatments. Next-generation sequencing has rapidly become the method of choice, owing to the high data yield and relatively low costs of data generation. To date, several reports have been published on the microbial diversity in contaminated soils analyzing the matrix's dynamics throughout different bioremediation processes via 16S-rRNA gene-fragment pyrosequencing (Lladó et al., 2013; Festa et al., 2016b).

Within this context, the aim of the present work was to evaluate the effect of a tandem remediation procedure combining ammonium-persulfate chemical oxidation with biological treatment on PAH elimination and the ecologic properties of soil material taken from a landfarming treatment done about twenty years ago. That original site is still now under natural attenuation at the petrochemical pole, Ensenada in La Plata.

It was hypothesized that a tandem oxidation-bioremediation treatment at low doses of persulfate could recover the microbial diversity and functionality of the oxidized soil. We decided to focus on a study of the changes in the soil bacterial-community composition produced during both steps, the persulfate addition and the bioremediation, using PCR-DGGE and the pyrosequencing of PCR-amplified bacterial 16S-rRNA gene fragments. Furthermore, to evaluate the changes in the organic matter and physiologic properties of the soil, the analysis by fluorescence–excitation–emission matrices (FEEMs) and measured the soil enzymatic activities were performed.

2. Materials and methods

2.1. Site description

The soil (S_0) was sampled from a chronically hydrocarbon-contaminated site, belonging to a petrochemical plant in a suburb of La Plata city, where some twenty years ago a landfarming treatment had been carried out. Approximately 20 kg of the first 20 cm of topsoil was collected from that site. That sample was sealed in a plastic bag and kept in the cold for transportation to the analytical laboratories so as to maintain the original moisture and thus preserve the microbial community. In the laboratory, the soil was thoroughly mixed and passed through a 2-mm sieve, then split into two samples for storage at 4 °C until the analyses. The soil was a loam (with 44.4% sand, 40.0% silt, and 15.6% clay along with a water-retention capacity of 27.5%). A soil from the same region as the S_0 sample, but without hydrocarbon contamination and thus designated S, was also removed as a control to compare the physicochemical properties with those of the contaminated soil.

2.2. Soil treatments

Two different treatments in the microcosms experiments were applied in the study.

2.2.1. Oxidative treatment with ammonium persulfate (OxS_0)

The ammonium persulfate (PS) concentration was calculated from the soil's oxidant demand (*i. e.*, 0.1 $kg_{PS} \cdot m^{-3}$ of dry soil; Osgerby, 2006) along with the amount of PS needed to mineralize each hydrocarbon species determined in S_0 . Approximately 15 kg of the contaminated soil (S_0) was oxidized with PS added as an aqueous solution by spraying (three applications per week) to reach the concentration $[PS]_0 = 33 \text{ g} \cdot \text{kg}^{-1}$ after 3 doses. Following each PS application the microcosms were mixed and then incubated at 30 °C for a further 7 days. The residual concentration of PS was determined after 7 and 37 days of treatment (Liang et al., 2008).

2.2.2. Bioremediation following oxidation ($BOxS$)

Of a sample from the oxidized soil (OxS_0), 500 g was incubated at 25 °C for 12 months. Microcosms containing the same quantity of the soil S_0 before the oxidative treatment were prepared and incubated for bioremediation in parallel as a control (BS). These two microcosms were mixed manually twice a week and water was added to maintain the moisture levels at 20–25% (v/w).

2.3. Soil analysis

2.3.1. Chemical and physical properties

The main physicochemical characteristics were analyzed according to standard techniques (Sparks, 1996) and in the text are abbreviated

as follows where indicated: pH, electrical conductivity (EC), and the contents of organic carbon, total nitrogen, available phosphorus (P) and iron (Fe), and total iron and sulfate.

2.3.2. Hydrocarbon content

Soil samples were extracted according to Environmental-Protection Agency (EPA) method 3550b, and analyzed for the hydrocarbon content by a gas chromatograph (Clarus 500, Perkin Elmer) equipped with a flame-ionization detector and a 5HT PE column (Perkin Elmer; length, 30 m; internal diameter, 0.25 mm). For aliphatic-hydrocarbon determination, samples were injected (1 μl) in the split mode (split ratio, 1:2) at 300 °C. The oven temperature was programmed from 60 °C (held for 2 min) to 170 °C at 10 °C·min⁻¹, then from 170 °C to 250 °C (held for 5 min) at 5 °C·min⁻¹. In addition, for determination of PAHs, the operating conditions were: an injection in the splitless mode at 250 °C with the oven temperature programmed from 80 °C (held for 1 min) to 140 °C at 25 °C·min⁻¹, then from 140 °C (held for 15 min) to 290 °C at 10 °C·min⁻¹. The temperature of the detector was 300 °C for both determinations. Helium was used as carrier gas (at 1 ml·min⁻¹ and 2 ml·min⁻¹, respectively). Each hydrocarbon concentration was determined by calibration with the corresponding standard (AccuStandar).

The bioavailable-PAH concentration from the chronically contaminated soil (S_0) was determined as previously described by Cébron et al. (2013) with XAD2 resin being used as the sorbent.

Triplicate samples at the end of the treatments were extracted with acetone/dichloromethane (1/1, v/v) as the solvent (Sayara et al., 2010) and quantified by gas chromatography (Del Del Panno et al., 2005).

2.3.3. Spectrofluorometric analysis of dissolved organic matter

The SOM was extracted according to Swift (1996) with minor modifications. The procedure stated in brief: 3 g of sample was stirred for 1 h with 15 mL of 0.1 M NaOH. The sediment was then separated by centrifugation, filtered through a membrane of pore size 0.45 μm , and the soluble fraction labelled as dissolved organic matter. These extracts were used for absorption-spectra analysis (E_4/E_6 ratio) and determination of the total dissolved carbon (DTC) and fluorescence–excitation–emission matrices (FEEMs). DTC was measured with a Total Organic Carbon Analyser Shimadzu, TOC5000 (Mora et al., 2009). The systems were characterized by the FEEM spectra determined with a computer-interfaced Near-IR Fluorolog-3 Research Spectrofluorometer (Birdwell and Engel, 2010). FEEMs were generated by recording successive emission spectra from 260 to 600 nm at excitation wavelengths ranging from 240 to 540 nm, with a 5-nm scan step. Excitation and emission slits were set to 5 nm (Bosio et al., 2008).

The parallel-factor analysis (PARAFAC) (Andersen and Bro, 2003) deconvolutes the information contained in a set of FEEMs into three matrices A (scores), B (emission loadings), and C (excitation loadings) for both quantitative and qualitative analysis (Su et al., 2015; Ballesteros et al., 2017). The three matrices contain the relative contribution profiles (A), the normalized emission spectra (B), and the normalized excitation spectra (C) for each of the factors that contribute to the observed signals in the solutions analyzed. The analysis was conducted with the MATLAB 7.7 software (Mathworks, Natick, MA) along with PLS_Toolbox version 4.0 (Eigenvector Research, Manson, WA). Several preprocessing steps were used before modeling to minimize the influence of scatter lines and other attributes of the FEEM that are caused by the background-solution matrix. A nonnegativity constraint was applied to the parameters to allow only the chemically relevant results. The correct number of factors was assessed by analysis of the physical sense of the spectral loadings and by evaluation of the distribution of residuals and additional model diagnostics.

2.3.4. Bacterial population density

A counting of the cultivable heterotrophic bacteria (HB) was carried out for each treatment. Samples (0.1 mL) at a 10-fold dilution were spread on plates containing R2A agar (Reasoner and Geldreich, 1985).

Inorganic phosphorus-solubilizing bacteria were counted after cultivation in phosphorus inorganic medium (Goldstein, 1986). Agar plates were incubated at (24 °C) for 10 days. The most probable number of aromatic- and aliphatic-hydrocarbon-degrading bacteria was determined in 96-well microtiter plates (Wrenn and Venosa, 1996) containing mineral-salts medium (Vecchioli et al., 1990), supplemented with the corresponding source of carbon. The inoculated microtiter plates were incubated at 24 °C for 21 days.

2.3.5. Enzymatic assays

Lipase (Margesin et al., 2002), urease (Kandler and Gerber, 1988), arylsulfatase (Whalen and Warman, 1996), and phosphatase (Verchot and Borelli, 2005) activities were determined before and after each treatment.

2.4. Genomic analysis

2.4.1. DNA extraction

Total DNA was extracted from 1-g aliquots of soil from each microcosm after treatment, by means of the E.Z.N.A.TM Soil DNA Isolation Kit (Omega Bio-tek, Inc., Norcross, GA, USA) according to the manufacturer's instructions. The quantity of DNA was measured with the Quant-iTTM PicoGreen[®] dsDNA Assay Kit (InvitrogenTM, Carlsbad, CA, USA).

2.4.2. 16S-rDNA, PCR, and DGGE analyses

A genetic-diversity analysis of the bacterial communities in the soil microcosms was performed by the PCR amplification of bacterial 16S ribosomal-DNA (rDNA) fragments followed by DGGE. The PCR was performed in duplicate, with DNA extracted from replicate microcosms. The 16S rDNA was amplified through the use of the eubacterial primers GC-341F and 907R (Muyzer et al., 1998). The PCR reactions were carried out as described (Festa et al., 2016a). The amplification was performed on a Mastercycler[®] Eppendorf thermocycler (Eppendorf, Wesseling-Berzdorf, Germany) by means of a step-down PCR. The PCR products were analyzed by electrophoresis on a 1.2% (w/w) agarose gel. The DGGE was carried out on a DGGE-2401 instrument (C.B.S Scientific Co., Del mar, CA, USA). The gel contained a linear gradient of 45–70% denaturant, with a 100% denaturant corresponding to 7 M urea in 40% (v/v) aqueous formamide.

After electrophoresis the gel was stained for 30 min with SYBR Gold, documented with a Chemidoc gel-documentation system (Bio-Rad, Hercules, CA, USA), and analyzed on the GelCompar II software package (Applied Maths, Kortrijk 180 Belgium). The similarity matrix was obtained by means of the GelCompar II software as described (Festa et al., 2016a).

2.4.3. DNA amplification and pyrosequencing

The PCR amplification of the 16S-rRNA gene was performed on each individual soil-DNA extraction with the universal bacterial primers,

341Fbac (Muyzer et al., 1993) and 909R (Tamaki et al., 2011) as described by Festa et al. (2016b) in order to amplify a 568-bp fragment of the gene flanking the V3 and V5 hypervariable regions. The amplicons from different samples were then mixed in equal concentrations and purified through the use of Agencourt Ampure beads (Agencourt Bioscience Corporation, MA, USA). The samples were next sequenced in a Roche 454 FLX with titanium instruments and reagents, following manufacturer's instructions. This sequencing was performed at the Molecular Research laboratory (MR DNA; Shallowater, TX) based on established and validated protocols (<http://www.mrdnalab.com/>).

2.4.4. Data analyses

The pyrosequencing data were analyzed by the Mothur software (version v.1.34.0; Schloss et al., 2009). Sequences were excluded from the analysis according to the criteria utilized by Fernández-González et al. (2017): The remaining sequences were denoised and the chimeras and contaminants removed by the Mothur software 454 SOP. The final sequence data were then clustered into Operational Taxonomic Units (OTUs) split by 3% genetic distance by means of the average-neighbor method. The OTUs were then taxonomically classified against SILVA nr 119, a database of high-quality small-subunit rRNA sequences for all three domains of life. In order to compare the relative differences among the samples, a randomly selected subset of 767 sequences per sample was performed for downstream analyses. For the statistical analysis of the data, Good's coverage index and the Hill numbers (species richness [H₀], the exponential of the Shannon diversity index [H₁] and the reciprocal of Simpson's index [H₂]; Hill, 1973), as calculated by the Mothur (version v.1.34.0) software (Liao et al., 2015), were used as measurements of species richness and diversity in accordance with current consensus (Jost, 2006; Chao et al., 2012). In order to analyze the changes in the microbial communities, a principal-component analysis (PCA) was performed with STAMP Software (v. 2.1.3; Parks et al., 2014).

2.5. Statistical analyses

The effect of the indicators evaluated during the treatments were interpreted by an analysis of variance (ANOVA) after the Tukey test with XLStat (v.7.5.2), at a significance threshold of $p < 0.05$.

3. Results

3.1. Effect of the treatments on the physicochemical properties of the soil and on hydrocarbon elimination

The pH, electrical conductivity and available P in S₀ were higher than in S, but the organic carbon and total nitrogen contents were similar in both soils (Table 1). The hydrocarbon contents determined for S₀ were 214 mg·kg⁻¹ of PAHs and 2460 mg·kg⁻¹ of aliphatic hydrocarbons (Table 2).

Table 1
Characteristics of the microcosm soils before and after the treatments^a.

| Microcosms ^a | S ₀ | OxS ₀ | BOxS | BS | S |
|--------------------------------|----------------|-------------------|-----------------|---------------|----------------|
| pH | 8.8 ± 0.1 (a) | 7.1 ± 0.1 (b) | 6.32 ± 0.02 (c) | 7.6 ± 0.1 (b) | 7.3 ± 0.2 (b) |
| EC [μS·cm ⁻¹] | 634 ± 12 (b) | 5110 ± 99 (a) | 5880 ± 396 (a) | 549 ± 42 (c) | 336 ± 1 (d) |
| OC [%] | 2.2 ± 0.8 (a) | 2.4 ± 0.1 (a) | 2.6 ± 0.1 (a) | 2.0 ± 0.9 (a) | 2.4 ± 0.3 (a) |
| TN [%] | 0.2 ± 0.1 (b) | 0.519 ± 0.003 (a) | 0.31 ± 0.04 (b) | 0.2 ± 0.1 (b) | 0.2 ± 0.1 (b) |
| P [mg·kg ⁻¹] | 8.3 ± 0.6 (c) | 14.5 ± 0.7 (b) | 22.0 ± 0.1 (a) | 6.0 ± 0.3 (d) | 3.67 ± 0.6 (e) |
| Fe [mg·kg ⁻¹] | 12.6 ± 0.3 (b) | 54 ± 2 (a) | nd | nd | nd |
| Sulfate [mg·kg ⁻¹] | 97 ± 6 (d) | 8407 ± 16 (a) | 4894 ± 15 (b) | nd | 154 ± 6 (c) |

For the same parameter, the mean values followed by different letters are significantly different ($p < 0.05$).

^a OxS₀, original contaminated soil, S₀, after oxidative treatment; BOxS original contaminated soil, S₀, after oxidative treatment and bioremediation in tandem; BS, original soil after bioremediation; S, uncontaminated soil from same region—these last two being controls for the experimental treatment; ds, dry soil; nd, not determined.

* EC, electrical conductivity; OC, organic carbon; TN, total nitrogen; P, available phosphorus; Fe, iron; and sulfate.

Table 2
Concentrations of hydrocarbons extracted from the microcosm soils.

| Microcosms ^a | S ₀ | OxS ₀ | BOxS | BS |
|-------------------------------------------------------------------------------------------------|----------------|------------------|---------------|----------------|
| Total polycyclic aromatic hydrocarbons (PAHs) [mg·kg _{ds} ⁻¹] ^b | 214 ± 21 (a) | 151 ± 12 (b) | 112 ± 4 (c) | 223 ± 12 (a) |
| 3-ring [%] | 35.6 | 27.0 | 17.7 | 31.7 |
| 4-ring [%] | 47.8 | 48.8 | 54.6 | 48.4 |
| 5-ring [%] | 6.2 | 6.5 | 9.8 | 7.3 |
| 6-ring [%] | 10.4 | 17.7 | 17.9 | 12.6 |
| Available PAHs [%] | 1 ± 1 (c) | 19 ± 4 (b) | 30 ± 2 (a) | 1 ± 1 (c) |
| Total aliphatic hydrocarbons [mg·kg _{ds} ⁻¹] ^c | 2457 ± 246 (a) | 2442 ± 182 (a) | 826 ± 172 (b) | 2978 ± 554 (a) |
| C ₉ -C ₂₀ [%] | 52.9 | 48.6 | 22.6 | 52.8 |
| C ₂₀ -C ₂₉ [%] | 42.1 | 43.5 | 68.8 | 41.4 |
| C ₂₉ -C ₃₅ [%] | 5.0 | 7.9 | 8.6 | 5.8 |

For the same parameter, the mean values followed by different letters are significantly different ($p < 0.05$).

^a OxS₀, original contaminated soil, S₀, after oxidative treatment; BOxS, original contaminated soil, S₀, after oxidative treatment and bioremediation in tandem; BS, original soil after bioremediation—control for the experimental treatment; ds, dry soil.

^b Soil PAH concentration and relative abundance of 2- to 6-ring PAHs in each microcosm, percentage of available PAHs extracted with the adsorbent XAD-2TM (sum of 16 US-EPA PAHs).

^c Soil Aliphatic-hydrocarbon concentration and relative abundance of low-, intermediate-, and high-molecular-weight hydrocarbons (C₉ to C₂₀; C₂₀ to C₂₉, and C₂₉ to C₃₅, respectively).

Table 3
Dissolved total carbon (DTC) and E₄/E₆ ratios for alkaline extracts from each microcosm.

| Microcosms ^a | S ₀ | OxS ₀ | BOxS | BS | S |
|--------------------------------|----------------|------------------|------------|----------------|-------------|
| DTC [mg·C·l ⁻¹] | 96 ± 3 (c) | 226 ± 2 (a) | 57 ± 2 (d) | 46.5 ± 0.8 (e) | 151 ± 2 (b) |
| E ₄ /E ₆ | 15.0 | 17.7 | 7.1 | 3.3 | 14.0 |

For the same parameter, the mean values followed by different letters are significantly different ($p < 0.05$).

^a OxS₀, original contaminated soil, S₀, after oxidative treatment; BOxS, original contaminated soil, S₀, after oxidative treatment and bioremediation in tandem; BS, original soil after bioremediation; S, uncontaminated soil from the same region—these last two, controls for the experimental treatment.

After oxidative treatment (OxS₀) the soil pH was reduced by almost one unit below the S₀ value. A significant increase in the sulfate, total available nitrogen, P, Fe, and EC was detected after the application of PS (Table 1). The oxidative treatment produced an elimination of 29% of the total PAHs, mainly represented by the 3-ring PAHs (Table 2). Moreover, the PS treatment released benzo[*g,h,i*]perylene from the soil matrix (data not shown) and increased the PAH bioavailability significantly, from 1% to 19%; but no elimination of aliphatic hydrocarbons was detected. After one month of the application, the PS concentration fell below the limit of detectability.

The combined treatment in tandem (BOxS) produced a decrease in the pH value; while a reduction in the total nitrogen and sulfate content

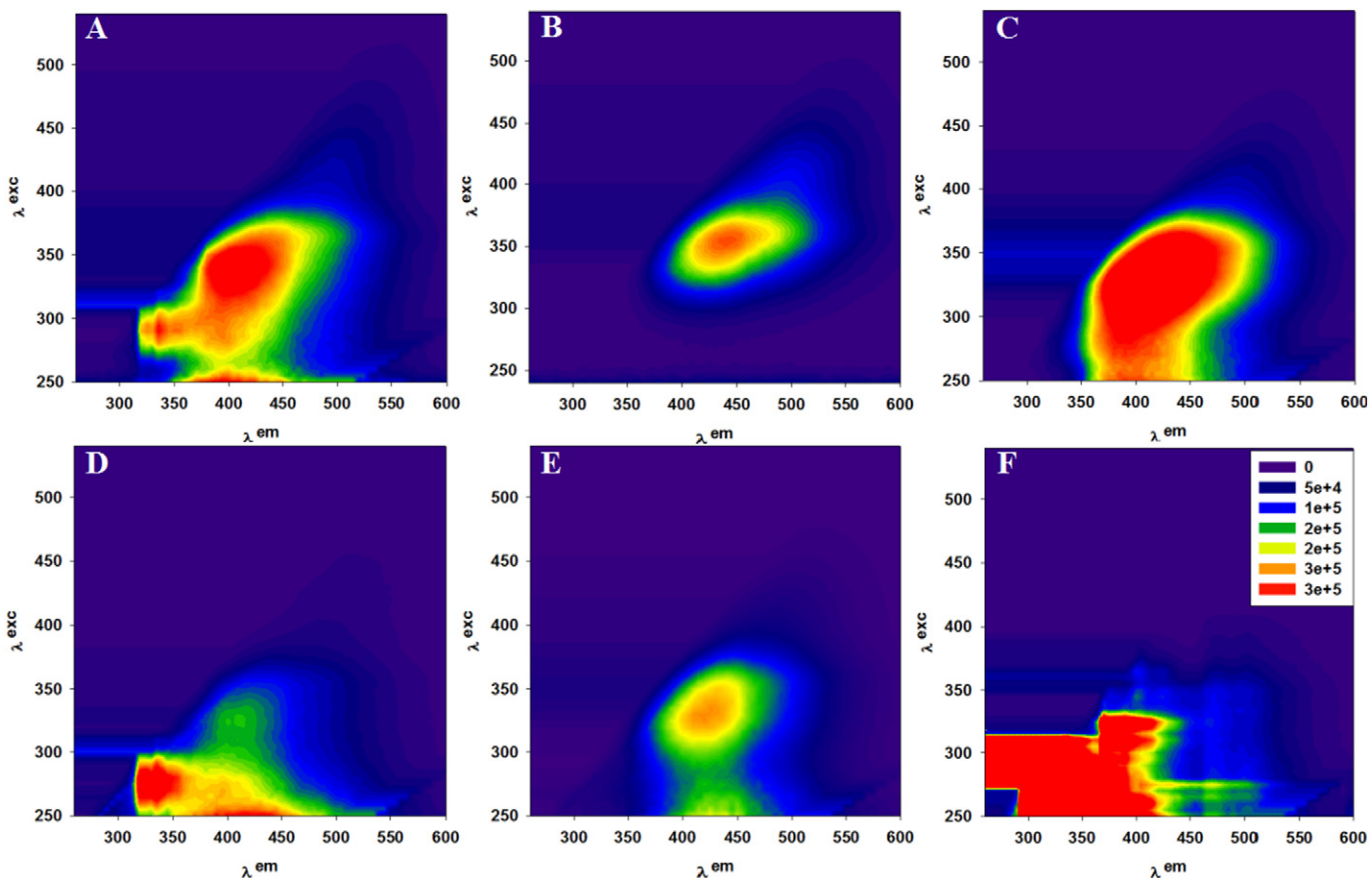


Fig. 1. Fluorescence-excitation-emission matrix (FEEM) for alkaline extracts from each microcosm. A. Contaminated soil (S₀). B. Oxidized soil (OxS₀). C. Bioremediated oxidized soil (BOxS). D. Bioremediated soil (BS). E. Control soil (S). F. Aqueous solution of 16 PAHs.

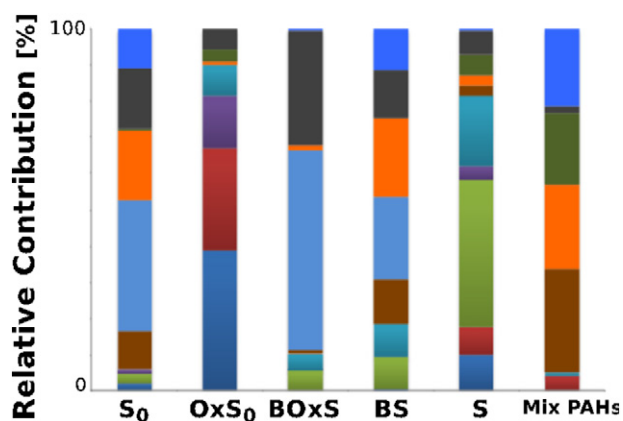


Fig. 2. Percent contribution of different fluorophores determined in the alkaline extract from each microcosm, including the control soil (S) and an aqueous solution of 16 PAHs (mix PAH).

was observed, with the available P content being increased and the EC remaining high (Table 1). About 26% of the PAHs were further eliminated in BOxS microcosms, mainly with respect to the 3- and 4-ring PAHs (Table 2). Moreover, the dibenzo[*a,h*]anthracene released from soil matrix became detectable (data not shown). The bioavailable-PAH fraction also increased, reaching 30%. A remarkable elimination of aliphatic hydrocarbons of around 66% was also detected, mainly owing to a decrease in the C₉–C₂₀ fraction (Table 2).

The bioremediation of the original contaminated soil (BS) had not produced changes in the properties of that soil, with the exception of a slight reduction in the pH and the available-P content. No significant changes in the content of either the aliphatic hydrocarbons or the PAHs were observed (Tables 1 and 2).

3.2. Spectroscopic properties of soil alkaline extracts

Table 3 lists the DTC and the E₄/E₆ ratio from the absorption spectrum of each alkaline extract. Fig. 1 depicts the FEEMs of the extracts from the S₀, OxS₀, BOxS, and BS microcosms. The FEEM of the extract of S (Fig. 1.E) and a solution of PAHs (Fig. 1.F) were included to identify the precedence of the fluorophore families.

The peaks at λ_{exc} 250–320 nm and λ_{em} < 380 nm (designated Region I) are related to PAHs (Vatsavai et al., 2008; Goicoechea et al., 2012; Merdy et al., 2014), while the peaks at λ_{exc} > 280 nm and λ_{em} > 380 nm (designated Region II) are assigned to humic acids from the soil (Bosio et al., 2008; Chen et al., 2003).

To analyze the contribution of each fluorophore family to the FEEM, a parallel-factor analysis was done. An optimal number of 13 factors were found to correctly describe the whole fluorescence set, with the lack of fit being lower than 1%. The shapes of the excitation and emission spectra for the deconvoluted factors are shown as Supplementary Material (Fig. S1). Fig. 2 summarizes the contribution of the fluorescence of each fluorophore family.

The FEEM from S₀ contained two regions with high fluorescence intensity, which can be associated with PAHs (Region I) and humic acids (Region II), as presented in Fig. 1.A. The DTC content of S₀ was slightly lower than that of S, and both soils showed similar E₄/E₆ ratios (Table 3).

The FEEM from OxS₀ (Fig. 1.B) indicated that the oxidative treatment decreased the PAH-associated fluorescence (Region I), and consequently the contribution to the total fluorescence (by <10%, cf. Figs. 2 and S2). These microcosms manifested a significant increase in the DTC in comparison to S₀, as the result of a nonspecific oxidation of the organic matter, without causing a significant change in E₄/E₆ ratio (Table 3).

A significant reduction in the DTC content was recorded in the BOxS microcosms as judged by an increase in the fluorescence of Region II (Fig. 1.C). Although the subsequent bioremediation modified neither the proportion of PAHs nor the contribution of the SOM to the total fluorescence, a different fluorophore distribution of the families within the SOM was obtained (Fig. 2).

Although Region II of the FEEM from BS was less intense than those of the other soil extracts (Fig. 1.D), a fluorophore distribution similar to that of S₀ was observed. In addition, both the DTC content and the E₄/E₆ ratio of the BS group were at the lowest values of all the microcosms (Table 3).

3.3. Effect of the treatments on the bacterial-population density and enzymatic activities of the soil

Fig. 3 shows the effect of the different treatments on the cultivable bacteria.

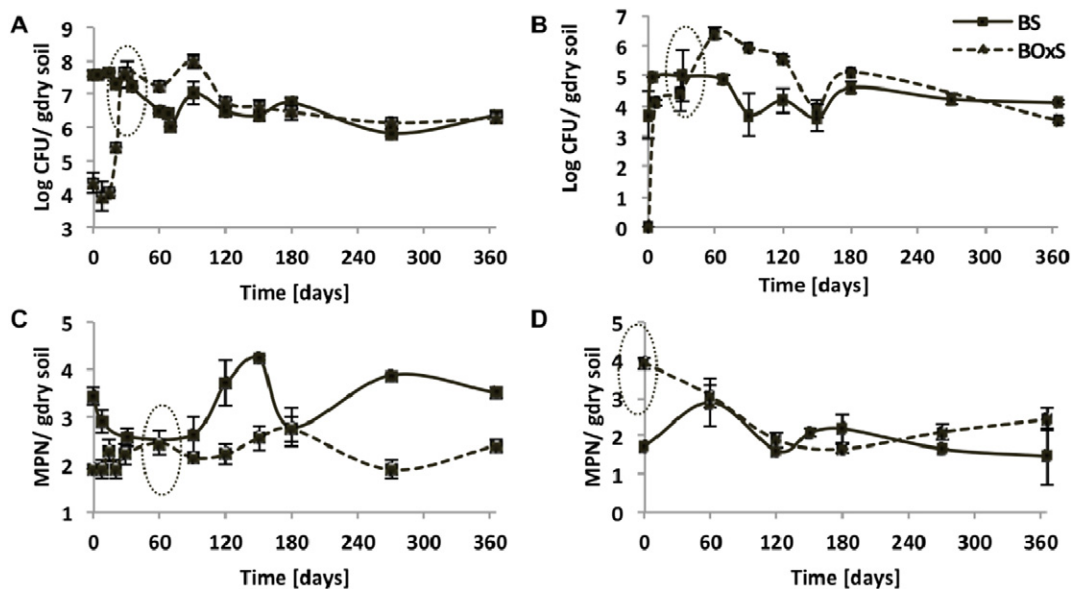


Fig. 3. Dynamics of populations of cultivable soil. A: Colony-forming units (CFUs) of heterotrophic bacteria. B: Colony-forming units (CFUs) of phosphorus-solubilizing bacteria. C: Most probable number (MPN) of polycyclic-aromatic-hydrocarbon-degrading bacteria. D: Most probable number (MPN) of aliphatic-hydrocarbon-degrading bacteria.

Table 4
Enzymatic activities determined for each microcosm.

| Microcosms ^a | S ₀ | OxS ₀ | BOxS | BS |
|------------------------------------------------------------------------------|----------------|------------------|--------------|--------------|
| Lipase [μg pNP · g _{ds} ⁻¹] | 189 ± 4 (b) | 267 ± 6 (a) | 114 ± 14 (c) | 174 ± 3 (b) |
| Arylsulfatase [μg pNP · g _{ds} ⁻¹] | 33 ± 1 (a) | 35 ± 1 (a) | nd | nd |
| Alkaline phosphatase [μg pNP · g _{ds} ⁻¹] | 175 ± 24 (b) | 84 ± 3 (c) | 157 ± 10 (b) | 303 ± 15 (a) |
| Acid phosphatase [μg pNP · g _{ds} ⁻¹] | 103 ± 20 (a) | 51 ± 6 (b) | nd | 42 ± 29 (b) |
| Urease [μN-NH ₄ ⁺ · g _{ds} ⁻¹] | 23 ± 6 (b) | nd | 204 ± 57 (a) | 17 ± 2 (b) |

For the same parameter, the mean values followed by different letters are significantly different ($p < 0.05$).

^a OxS₀, original contaminated soil, S₀, after oxidative treatment; BOxS, original contaminated soil, S₀, after oxidative treatment and bioremediation in tandem; BS, original soil after bioremediation; ds, dry soil; nd, not detected.

A dramatic decrease of about three orders of magnitude was observed in the HB population and in the PAH-degrading bacteria originally in S₀ after the oxidative treatment of the OxS₀ microcosms. Moreover, the population of phosphorus-solubilizing bacteria became undetectable. In contrast, a significant increase in the population of AH-degrading bacteria occurred (Fig. 3).

After the oxidative treatment, the only enzymatic activity significantly increased was the lipase. In contrast, the arylsulfatase activity was not affected, while the alkaline- and acid-phosphatase activities became diminished. The loss of urease activity was attributed to the product inhibition effect by the ammonium persulfate addition (Table 4).

A fast recovery of the HB population was observed during the combined treatment (BOxS, Fig. 3.A). The population reached a density similar to that detected in the BS microcosms in a month, and temporarily surpassed that value at about 100 days. Evidence of the phosphorus-solubilizing capability of the bacterial population was registered during the first week of the bioremediation treatment (BOxS). Later, that activity increased and remained higher than in the BS microcosms during nearly the next four months (Fig. 3.B). The significantly reduced population of PAH-degrading bacteria after the oxidation never recovered throughout the following bioremediation (Fig. 3.C), whereas the initially increased population of aliphatic-hydrocarbon-degrading bacteria subsequently declined during the next two months of bioremediation and remained low thereafter (Fig. 3.D).

After the combined in-tandem treatment of the BOxS₀ microcosms, the lipase activity decreased during the bioremediation to a value lower than that in BS microcosms, whereas the urease and alkaline-phosphatase activities were recovered. The arylsulfatase activity was not detected in either the BOxS₀ or the BS₀ microcosms (Table 4).

3.4. Effect of the treatments on the soil bacterial community

3.4.1. Community structure

The comparison of the DGGE patterns revealed significant changes in the structure of the bacterial-communities in the oxidized soil during the coupled bioremediation treatment (Fig. 4). One change was characterized by a clustering of the patterns from the oxidized soil briefly exposed to bioremediation (similarity of 82%) and represented the early changes in the soil-bacterial community. The other by a clustering of the patterns from the oxidized soil exposed to a longer time of bioremediation (similarity of 70%), representing the later changes in the soil-bacterial community. The patterns from OxS₀ were clustered with that representing the earlier changes, and the patterns from the S₀ were grouped with that representing the later community changes.

On the basis of these dendrograms, different times during the bioremediation were selected from which the pyrosequencing analyses of the bacteria from the soil microcosms were performed.

3.4.2. Bacterial composition: General analysis of the pyrosequencing data set

The taxonomic composition and diversity of the bacterial communities of the microcosm OxS₀ and after 1, 5, 9, and 12 months of subsequent bioremediation were profiled by pyrosequencing. Soil samples from the S₀ and BS microcosms were also analyzed for comparison as controls.

The pyrosequencing-based analysis and subsequent statistical inference provided 17,944 prokaryotic sequences (at an average length of 389 bp) after the data trimming. The sequence file was submitted to the National Center for Biotechnology Information Sequence Read Archive (www.ncbi.nlm.nih.gov/sra) and is available at the accession number SRP068448.

The Good's coverage in all the samples was over 84%. The rarefaction curves corresponding to samples from BOxS taken at 9 and 12 months and samples from S₀ and BS did not approach saturation, indicating

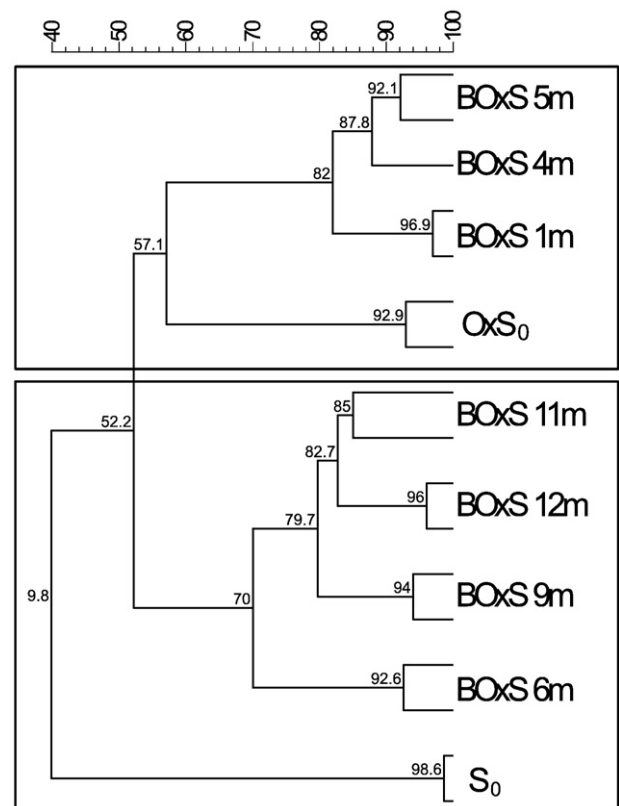


Fig. 4. The neighbor-joining tree based on a distance-matrix analysis of 16S-rDNA DGGE bands was constructed by means of the GelComparII software package.

that their microbial communities were highly complex (Fig. 5.A). These rarefaction curves estimating the OTU richness confirmed the difference between the soil samples from the S_0 , and experimental microcosms after the various treatments (Table 5), where S_0 and BOxS (at 9 and 12 months) were predicted to have a higher degree of microbial-species richness than the other soil samples.

A dramatic decline in species richness (H_0) was observed in the Ox S_0 microcosms. The new community contained an uneven assemblage (H_2) with less species diversity (H_1). This pattern was exacerbated as a result of the subsequent bioremediation over the first five months. Although the diversity (H_1) and equitability (H_2) indices were recovered in the soil community after the ninth month of

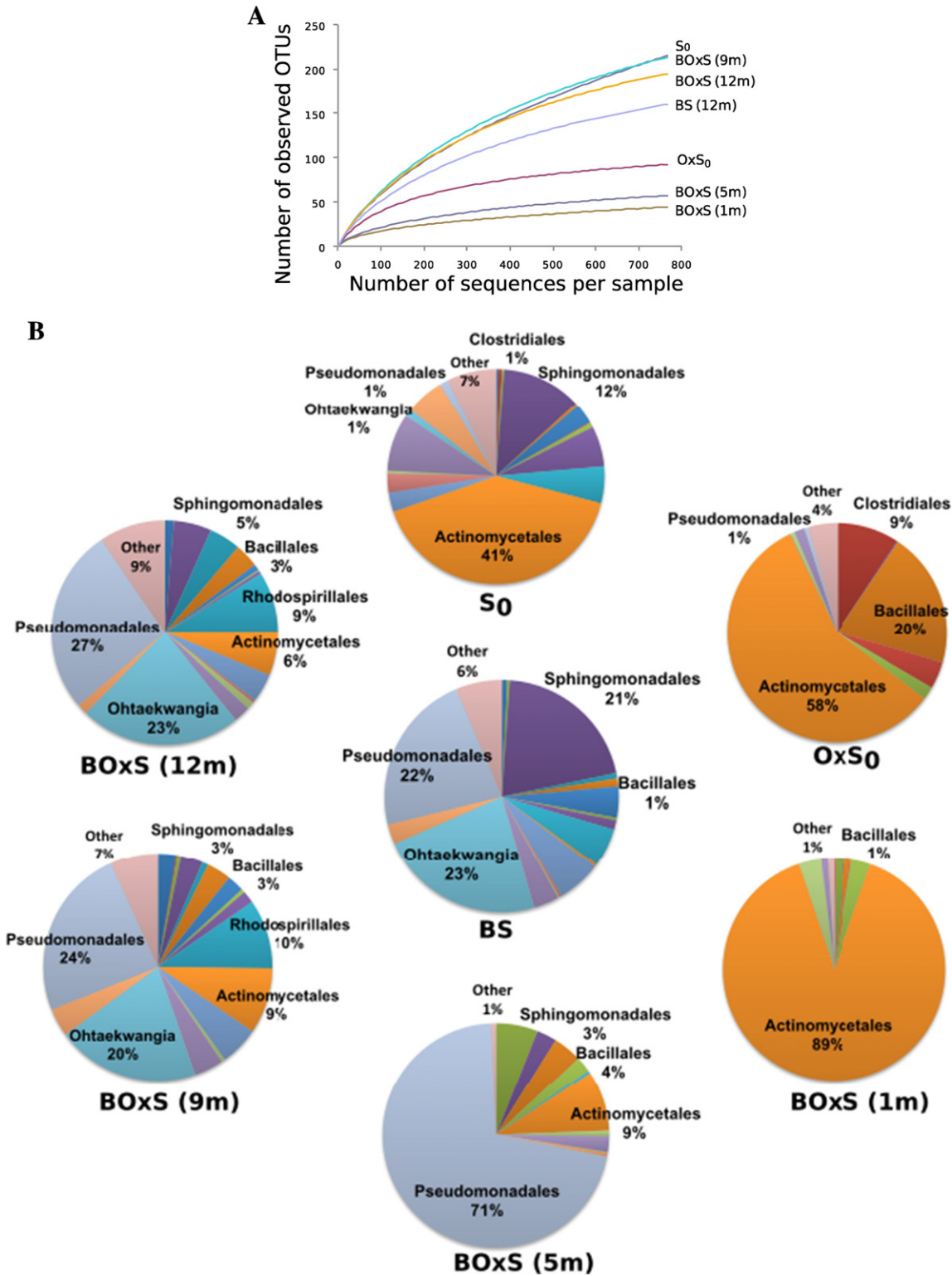


Fig. 5. A. Rarefaction analysis constructed by means of the Mothur v.1.34.0 software. In the figure, the rarefaction curves for the S_0 , Ox S_0 , BOxS, and BS microcosms are plotted. B. Pie diagrams illustrating the relative phylotype frequency at the level of order as revealed by pyrosequencing. The affiliation was determined by using the classifier command of Mothur against a curated Ribosomal Database Project (RDP). The orders with <5% reads belonging to each class were grouped in the sector labelled Other.

bioremediation, the combined treatment failed to recover the species richness (H_0 ; Table 5).

The diversity and richness estimators described by Hill (1973) in the soil community from the BS microcosms suggested that the bioremediation treatment had resulted in—after a year's time—the selection of a less rich community with a similar, though somewhat lower, species diversity; but the most common species were nevertheless present in a slight prevalence, albeit at an unequal assemblage.

3.4.3. Effect of the treatments on bacterial diversity

All the sequences were found to be classified within the domain Bacteria. Fig. 5.B summarizes the relative abundance of the different orders identified in each microcosm.

Members of the orders Actinomycetales (40.5%) and Sphingomonadales (12.0%) represented the bacterial community of S_0 , with *Nocardioide*s, *Mycobacterium*, *Actinophytocola*, and *Sphingomonas* being the most representative genera.

The oxidative treatment produced a loss of species richness leaving a community dominated by members of Actinomycetales (57.6%), with *Streptomyces* as the most abundant genus. In the microcosms of OxS_0 , however, the orders Bacillales (20.0%) and Clostridiales (9.3%) were also detected in a lower proportion.

Successional changes in the soil's resident community occurred during the course of the bioremediation treatment in BOxS. After one month, the abundance of members of Actinomycetales order increased up to a value of 89.5%, with a predominance of members of the genus *Cellulosimicrobium*. The low species richness and uneven assemblage, however, remained until the fifth month, though with Pseudomonadales as the predominant order (71.2%) and *Acinetobacter* as the major genus.

A notable recovery of richness and diversity from the bacterial community resulted after 9 months represented by members of the orders Pseudomonadales (24.3%) and Ohtaekwangia (20.2%), but with members of the *Acinetobacter* genus still remaining as predominant. The high profile of *Acinetobacter* continued until 12 months, with the genera *Sphingomonas* and *Bacillus* being present in lower proportions by that time.

The pyrosequencing analyses from the BS microcosms revealed a predominance of members of Ohtaekwangia (22.9%) along with Pseudomonadales (22.5%) and Sphingomonadales (20.6%). *Acinetobacter* and *Sphingomonas* were the most abundant genera identified in this microcosm.

Fig. 6 represents the PCA from the bacterial community at the taxonomic level of order of S_0 , BS, OxS_0 , and BOxS along with the sampling time during the subsequent bioremediation treatment in the last of those microcosms. An explained variance of 93.1% was obtained. The figure indicates that the S_0 , OxS_0 , and BOxS (1-month) microcosms

Table 5
Pyrosequencing-based analysis of the different communities studied^a.

| Microcosms ^a | Total sequences | Observed OTUs | Good's Coverage [%] | H_0 | H_1 | H_2 |
|-------------------------|-----------------|---------------|---------------------|-------|-------|-------|
| S_0 | 5984 | 215 | 84 | 449 | 61 | 44 |
| OxS_0 | 3404 | 92 | 97 | 112 | 28 | 10 |
| BOxS (1 m) | 4878 | 44 | 97 | 65 | 6 | 3 |
| BOxS (5 m) | 1094 | 57 | 97 | 71 | 8 | 4 |
| BOxS (9 m) | 959 | 213 | 88 | 286 | 64 | 49 |
| BOxS (12 m) | 767 | 194 | 91 | 234 | 60 | 40 |
| BS (12 m) | 858 | 160 | 92 | 216 | 47 | 28 |

^a The number of total sequences, observed OTUs clustered at a 97%-similarity level, Good's coverage (i. e., Hill numbers), H_0 (species richness), H_1 (the exponential of the Shannon diversity) and H_2 (the reciprocal of Simpson's index) for the different communities studied, were calculated through the use of a randomly selected subset of 767 sequences per sample. The bioremediation of the original soil (BS) was taken as control treatment.

^a OxS_0 , original contaminated soil, S_0 , after oxidative treatment; BOxS original contaminated soil, S_0 , after oxidative treatment and bioremediation in tandem; BS, original soil after bioremediation.

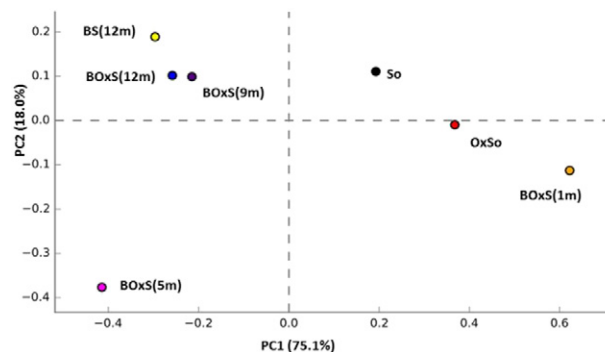


Fig. 6. Principal-component-analysis (PCA) plot. Comparison of the bacterial-community taxonomic profiles from each microcosm at the level of order, including those of the microcosms of BS. The analysis based on the relative abundance of orders was made with the STAMP software (v 2.1.3).

shifted to the right of the PC1 axis, thus implying the abundance of members of Actinomycetales and Pseudomonadales orders. The presence of members of the order Ohtaekwangia mainly pointed out the difference between the bacterial communities from OxS_0 up to the fifth month (constituting the early changes) from those incubated after nine months until the end of the bioremediation treatment, including BS (consisting in the later changes) on the PC2 axis.

4. Discussion

4.1. Implications of the oxidative treatment

Few studies on the remediation of PAH-contaminated soil through the direct application of PS to the soil have been recently published (e. g., Mora et al., 2014). In the one cited, however, the authors, applied the oxidative treatment to microcosms having soil that was contaminated with only one PAH (i. e., phenanthrene). The batch (slurry) (Lemaire et al., 2013b; Sutton et al., 2014a; Peluffo et al., 2015; Pardo et al., 2015) and the continuous-flow column (Richardson et al., 2011; Lemaire et al., 2013a) have been the most frequently studied systems to evaluate the efficiency of chemical oxidation on soil-hydrocarbon elimination. In addition, a variety of protocols have been applied, making a comparison of the results difficult.

Applying a PS dose similar to that used in the present work, Richardson et al. (2011), however, did not observe a PAH elimination from a chronically PAH-contaminated soil. The authors attributed that failure to the reduced soil-PAH availability and severely questioned the applicability of PS to the oxidation of highly weathered contaminants. Conversely, from our results, the low PAH bioavailability determined in S_0 did not hamper the elimination of PAHs after the oxidative treatment.

Moreover, after PS addition the bioavailable fraction increased along with a significant enhancement in the available nutrients such as DTC, Fe, and P. Numerous studies have suggested that the chemical oxidation of the SOM releases nutrients (Westersund et al., 2006; Sirguyev et al., 2008; Sutton et al., 2014b; Sutton et al., 2014c) and in so doing develops a new environment for the surviving microbial community. In contrast, alkaline extracts from the soil after the oxidative treatment exhibited an E_4/E_6 ratio similar to that of S_0 -soil extracts, thus suggesting that no remarkable changes were produced in the nature of the humic substances by the PS oxidation. Nevertheless, the fluorescence analysis manifested the disappearance of the region assigned to PAHs as part of a major change in the fluorophore profile; while, in addition, a desorption of PAH from the soil matrix was suggested by an increase in the concentration of benzo[*g,h,i*]perylene.

Furthermore, after PS addition a differential effect on the hydrocarbon-degrading populations was observed in the form of a reduction in the PAH degraders along with an increase in the aliphatic-

hydrocarbon degraders, pointing to a resistance to the negative effects of chemical oxidation in the latter. The decrease in the sensitive population and the increase in DTC could confer a competitive advantage on the aliphatic-hydrocarbon degraders in that oxidized soil, while the increase in lipase—the only enzymatic activity that was stimulated—was, for its part, an indicator of hydrocarbon biodegradation (Margesin et al., 1999). Nevertheless, the higher sulfate concentrations remaining in that soil certainly could influence microbial rebound.

4.2. Implications of the combined treatment

The bioremediation following the oxidative treatment produced an additional PAH elimination along with an increase in the bioavailable fraction. This pattern suggested that a dynamic of hydrocarbon desorption driven by the microorganisms had enabled a new PAH fraction to become available. In addition, an increase in the dibenzo[*a,h*]anthracene content and the higher contribution of SOM to the relative fluorescence (as part of a new fluorophore profile), in comparison to those properties in the BS soil, indicated that changes in the soil matrix produced by the microbial process had occurred throughout the bioremediation after the oxidation.

As Shirshova et al. (2006) suggested, the E_4/E_6 ratio is indicative of the molecular size, condensation, and aromatization of humic acids. Accordingly, the lower E_4/E_6 ratio determined after the combined treatment would be associated with the characteristic of a high relative molecular size and degree of condensation in the organic compounds, which feature implied a maturation of the SOM.

The DTC mobilized during the oxidation was consumed throughout the aliphatic-hydrocarbon degradation (principally owing to the low-molecular-weight fraction), thus suggesting that cometabolic effects could have promoted the hydrocarbon elimination. The activities of lipase, alkaline phosphatase, and urease detected after a year of bioremediation could be related to that microbial activity. Similar results were observed by Sutton et al. (2014a), who concluded that the biologic utilization of mobilized nutrients conditions the success of bioremediation coupled oxidation treatments.

The reduction in both the total hydrocarbons and the DTC after the combined treatment were accompanied by changes in the bacterial populations. The heterotrophic and the phosphorus-solubilizing bacteria were increased during the first months of the treatment, evidencing their resilience behavior as active generalist consumers in the autochthonous soil community. Unlike this response, the PAH degraders failed to recover during bioremediation, suggesting a marked sensitivity to the oxidative treatment; while the aliphatic-hydrocarbon degraders alone manifested a tolerance to PS oxidation. Through quantitative PCR, Richardson et al. (2011) had observed a similar response pattern and argued that resilience might be a function of group-specific tolerance to oxidative conditions.

4.3. Inferences from the dynamics of soil bacterial diversity

With the objective of bypassing the limitations of bacterial cultivation in the attempt to understand the contribution of the microbial community to the different treatments, the analysis by DGGE of the community profiles and taxonomic compositions during the bioremediation following the oxidative treatment were done.

The early changes in the community structure after oxidative treatment correlated with a successive reduction in the diversity indices, suggesting the loss of richness and species diversity characteristic of the S_0 , along with the establishment of a community with few predominant members. At about the sixth month, a gradual shift in the bacterial community reverted to an arrangement similar to that observed before the oxidative treatment (*i. e.*, constituting the later changes). The species richness, however, became reduced to 50% of that in the original soil (S_0), and a similar reduction in the number of species was recorded in the soil after a year of bioremediation (BS), but a less diverse and less

unequal arrangement was reached. Since the contaminated soil, S_0 was the same in both the BOxS and BS, microcosms, the similarity in H_0 values (species richness) of those two soils reached towards the end of the bioremediation in the former evidenced the resistance and resilience of the soil-community members that had been subjected to that oxidative stress.

The abundance of *Actinomycetales* in S_0 was replaced in OxS_0 by members of the *Streptomyces* genus (high-GC-content group) and members of the orders Bacillales and Clostridiales (low-GC group) in a lower proportion. This selection suggests a degree of sensitivity on the part of the microorganisms to oxidative conditions and to exposure to reactive oxygen species. Therefore, those bacteria had to have developed different strategies to cope with the oxidative stress. *Streptomyces coelicolor* has been extensively studied with respect to the role of the species's sigma factors in coordinate gene expression in response to environmental conditions in order to confront osmotic and oxidative stress (Lee et al., 2005). Recently, a novel strain *Streptomyces antioxidans* MUSC164T recovered from soil displayed potent antioxidative and neuroprotective activities against hydrogen peroxide (Ser et al., 2016). In addition, members of Bacillales and Clostridiales have been described as possessing, in addition to their sporulation capability, a variety of mechanisms to confront adverse environmental conditions such as acid, osmotic, and oxidative stresses (Zuber, 2009; Venkataramanan et al., 2013).

The initial abundance of the Actinomycetales order gradually increased during the first months of tandem bioremediation, but the *Streptomyces* dominance was replaced by members of *Cellulosimicrobium* genus. A notable shift in the order of dominance was detected after the fifth month represented by members of *Acinetobacter* (Pseudomonadales), maintaining an unequal community arrangement.

These successional changes could be explained through the so-called *r-K* scheme (Atlas and Bartha, 1998). In the presence of high concentrations of resources, as suggested by the increased levels of DTC, only resistant bacteria could survive when faced with oxidative-stress conditions. Contrary to the usual assumption that Streptomyces tend to be more successful in resource-limited situations as K strategists (Lebeau, 2011), the prevalence of that order after the oxidative treatment could be attributed both to the resistance capability of *Streptomyces* and to the lack of competition. Species from the genus *Cellulosimicrobium* have been isolated from different environments, including soil (Yoon et al., 2007). Antony et al. (2009) isolated a *C. cellulans* strain from Antarctic soil, which isolate evidenced a highly flexible metabolic activity with a greater preference for utilizing complex, high-molecular-weight carbon substrates. Those properties would confer a competitive advantage on *Cellulosimicrobium* cells during the early phase of bioremediation, thus enabling the inclusion of that genus in the K-strategist category.

The rebound of members of the *Acinetobacter* genus signalled a change in the community from the K to an *r* strategy after five months. *Acinetobacter* strains are frequently isolated from both pristine and contaminated soils (Chen et al., 2012; Jung and Park, 2015). Owing to a great catabolic versatility, the abundance of species of this genus has suggested their active participation in the nutrient cycle during bioremediation. Considering that the heterotrophic nitrifying microorganisms are widely distributed in the soil it is possible to assume that *Acinetobacter* strains could have contributed to a reduction in the soil nitrogen content because of their denitrifying capability even under oxic conditions (Zhu et al., 2012).

The dominance of *Acinetobacter* was slowly decreasing, while the presence of taxa from other phyla—such as Ohtaekwangia, Rhodospirillales, and Actinomycetales—determined the establishment of a more equitable community towards the end of the treatment. Ohtaekwangia appeared as a relevant order from the time of the ninth month of bioremediation after oxidative treatment and increased up to an abundance of 23% at the end of one year. Ohtaekwangia strains

have been investigated as potential petroleum-hydrocarbon degraders, and one strain was reported to be involved in PAH degradation (McGenity et al., 2012). Moreover, Rhodospirillales became increased in relative abundance (up to ~10%) towards the end of this treatment. Members of the Rhodospirillales have demonstrated the ability to perform an aerobic phototrophic sulfate reduction in addition to exhibiting heterotrophy (Madigan, 2005; Rodrigues-Diaz et al., 2008). The higher sulfate concentration remaining after the oxidation could well constitute a negative feature of the oxidative treatment, but the relative abundance of members of the Rhodospirillales order, along with other recognized sulfate reducers under oxic conditions, could have contributed to a decrease in the sulfate observed during the bioremediation. Moreover, two genera of Rhodospirillales (*Azospirillum* sp. and *Phaeospirillum* sp.) have been found in hydrocarbon-contaminated soils (Abbasian et al., 2016).

The abundance of the Sphingomonadales in the soil of the solely bioremediated microcosm BS revealed the difference between this microcosm and the one subjected to the combined treatment, BOxS. In spite of the abundance of the recognized hydrocarbon-degrading members of the *Sphingomonas* (Coppotelli et al., 2008; Jouanneau et al., 2016) and *Acinetobacter* (Seo et al., 2009) genera, that BS microcosm evidenced no elimination of hydrocarbons, suggesting that the low PAH bioavailability and the organic-matter content were not sufficient to promote active hydrocarbon biodegradation. Instead, the significant DTC consumption and the evident organic-matter transformation indicated an active microbiologic contribution to the biogeochemical cycle of the organic matter.

The changes in the diversity and ratios of the microorganisms after the coupled treatment denoted a shift into the physiology of the microbial community throughout the tandem bioremediation, with that process becoming more diverse towards the end of the treatment. According to ecological and evolutionary theory, diverse communities provide a larger contribution to ecosystem functions and service compared to the less diverse counterparts (Bell et al., 2005). Although the bacterial-soil richness was partially recovered in both the microcosms BOxS and BS, the arrangement of relatively greater equality observed in the BOxS suggests a contribution of a higher number of species to the organic-matter cycling, as a result of the input of available nutrients produced by the oxidative treatment.

5. Conclusion

The results of applying PS to a long-term contaminated soil from a landfarming unit, indicated a significant PAH elimination in soil-microcosm experiments.

Although a significant impact on the microbial community was evidenced, a subsequent bioremediation treatment in tandem enabled the microbial population to recover along with an additional elimination of PAHs and aliphatic hydrocarbons. The reduction in the E_4/E_6 ratio from the DTC-mobilized fraction demonstrated the active metabolic capability of the resistant populations during the coupled bioremediation. Moreover, the mobilized nutrients and the increased PAH bioavailability promoted a cometabolic elimination of the hydrocarbons. Even though the combined treatment resulted in a loss of richness, the final established community was found to be similar to that observed when only the bioremediation treatment had been applied, suggesting that the higher sulfate concentration after the oxidative treatment would not be an impediment to the recovery of the bacterial community.

Spectroscopic analysis became a useful tool to follow and compare the different remediation treatments involving acute changes in the matrix of chronically hydrocarbon-contaminated soils. The high-throughput-DNA-sequencing techniques enabled an identification of the population dynamics of the predominant taxa that could be associated with the changes observed as result of the treatments.

These findings prompt a consideration of the coupling other kinds of bioremediation strategies—such as composting; which approach,

through the input of an active biomass and organic material, could promote an enhancement in hydrocarbon elimination and a faster recovery of the soil's properties.

Acknowledgements

The authors thank Dr. Fernando S. García Einschlag from INIFTA, for fruitful comments and suggestions in parallel-factor analysis. This research was partially supported by the Agencia Nacional de Promoción Científica y Tecnológica (PICT 2010–00366) and PIO 2014–2015–1332013010005CO. Rocío Medina has a postdoctoral fellowship supported by CONICET. Pedro Maximiliano David Gara is research member of CIC-PBA, Antonio José Fernández-González is member of Université de Lorraine, Interactions Arbres–Microorganismes (INRA, Interactions Arbres–Microorganismes, France), Janina Alejandra Rosso is research member of CONICET and María Teresa Del Panno is research member of Universidad Nacional de La Plata. Dr. Donald F. Haggerty, a retired career academic investigator and native English speaker, edited the final version of the manuscript.

Appendix A. Supplementary data

Supplementary data to this article can be found online at <https://doi.org/10.1016/j.scitotenv.2017.10.326>.

References

- Abbasian, F., Lockington, R., Megharaj, M., Naidu, R., 2016. The biodiversity changes in the microbial population of soils contaminated with crude oil. *Curr. Microbiol.* 72 (6): 663–670. <https://doi.org/10.1007/s00284-016-1001-4> (Springer US).
- Abdel-Shafy, H.I., Mansour, M.S.M., 2015. A review on polycyclic aromatic hydrocarbons: source, environmental impact, effect on human health and remediation. *Egypt. J. Pet.* 25 (1):107–123. <https://doi.org/10.1016/j.ejpe.2015.03.011> (Egyptian Petroleum Research Institute).
- Akkanen, J., Tuikka, A., Kukkonen, J.V.K., 2012. On the borderline of dissolved and particulate organic matter: partitioning and bioavailability of polycyclic aromatic hydrocarbons. *Ecotoxicol. Environ. Saf.* 78:91–98. <https://doi.org/10.1016/j.ecoenv.2011.11.010>.
- Andersen, C.M., Bro, R., 2003. Practical aspects of PARAFAC modeling of fluorescence excitation-emission data. *J. Chemom.* 17 (4):200–215. <https://doi.org/10.1002/cem.790>.
- Andrade-Eiroa, Á., Canle, M., Cerdá, V., 2013. Environmental applications of excitation-emission spectrofluorimetry: an in-depth review II. *Appl. Spectrosc. Rev.* 48 (2): 77–141. <https://doi.org/10.1080/05704928.2012.692105>.
- Antony, R., Krishnan, K.P., Thomas, S., Abraham, W.P., Thamban, M., 2009. Phenotypic and molecular identification of cellulose-degrading microorganisms isolated from Antarctic snow. *Antonie Van Leeuwenhoek* 96 (4), 627.
- Asquith, E.A., Geary, P.M., Nolan, A.L., Evans, C.A., 2012. Comparative bioremediation of petroleum hydrocarbon-contaminated soil by biostimulation, bioaugmentation and surfactant addition. *J. Environ. Sci. Eng.* 1 (5), 637–650.
- Atlas, R.M., Bartha, R., 1998. *Microbial Ecology: Fundamentals and Applications*. 4th ed. Benjamin/Cummings Publishing, Menlo Park, Calif.
- Ballesteros, S., García, M., Costante, R., Vicente, M., Mora, A., Amat, M., Arques, A., Carlos, L., García Einschlag, F.S., 2017. Humic-like substances from urban waste as auxiliaries for photo-fenton treatment: a fluorescence EEM-PARAFAC study. *Photochem. Photobiol. Sci.* 16 (1):38–45. <https://doi.org/10.1039/C6PP00236F>.
- Bamforth, S.M., Singleton, I., 2005. Bioremediation of polycyclic aromatic hydrocarbons: current knowledge and future directions. *J. Chem. Technol. Biotechnol.* 80 (7): 723–736. <https://doi.org/10.1002/jctb.1276>.
- Bell, T., Newman, J.A., Silverman, B.W., Turner, S.L., Lilley, A.K., 2005. The contribution of species richness and composition to bacterial services. *Nature* 436, 1157–1160.
- Birdwell, J.E., Engel, A.S., 2010. Characterization of dissolved organic matter in cave and spring waters using UV-vis absorbance and fluorescence spectroscopy. *Org. Geochem.* 41 (3):270–280. <https://doi.org/10.1016/j.orggeochem.2009.11.002>.
- Bosio, G.N., David Gara, P.M., Einschlag, F.S., Gonzalez, M.C., Del Panno, M.T., Martire, D.O., 2008. Photodegradation of soil organic matter and its effect on gram-negative bacterial growth. *Photochem. Photobiol.* 84 (5):1126–1132 (doi:PH274 [pii])[\[r\]https://doi.org/10.1111/j.1751-1097.2007.00274.x](https://doi.org/10.1111/j.1751-1097.2007.00274.x)).
- Cébron, A., Faure, P., Lorgeoux, C., Ouvrard, S., Leyval, C., 2013. Experimental increase in availability of a PAH complex organic contamination from an aged contaminated soil: consequences on biodegradation. *Environ. Pollut.* 177:98–105. <https://doi.org/10.1016/j.envpol.2013.01.043>.
- Chao, A., Chiu, C.H., Hsieh, T.C., Inouye, B.D., 2012. Proposing a resolution to debates on diversity partitioning. *Ecology* 93 (9):2037–2051. <https://doi.org/10.1890/11-1817.1>.
- Chen, J., LeBoeuf, E.J., Dai, S., Gu, B., 2003. Fluorescence spectroscopic studies of natural organic matter fractions. *Chemosphere* 50, 639–647.
- Chen, J., Huang, P.T., Zhang, K.Y., Ding, F.R., 2012. Isolation of biosurfactant producers, optimization of P. T. and properties of biosurfactant produced by *Acinetobacter* Sp. from

- petroleum-contaminated soil. *J. Appl. Microbiol.* 112 (4):660–671. <https://doi.org/10.1111/j.1365-2672.2012.05242.x>.
- Coble, P.G., 1996. Characterization of marine and terrestrial DOM in seawater using excitation-emission matrix spectroscopy. *Mar. Chem.* 51 (4):325–346. [https://doi.org/10.1016/0304-4203\(95\)00062-3](https://doi.org/10.1016/0304-4203(95)00062-3).
- Coppotelli, B.M., Ibarrolaza, A., Del Panno, M.T., Morelli, I.S., 2008. Effects of the inoculant strain *Sphingomonas paucimobilis* 20006FA on soil bacterial community and biodegradation in phenanthrene-contaminated soil. *Microb. Ecol.* 55 (2):173–183. <https://doi.org/10.1007/s00248-007-9265-7>.
- Cory, R.M., Miller, M.P., McKnight, D.M., Guerard, J.J., Miller, P.L., 2010. Effect of instrument-specific response on the analysis of fulvic acid fluorescence spectra. *Limnol. Oceanogr. Methods* 8 (2):67–78. <https://doi.org/10.4319/lom.2010.8.67>.
- Dabestani, R., Ivanov, I.N., 1999. Invited review a compilation of physical, spectroscopic and photophysical properties of polycyclic aromatic hydrocarbons. *Photochem. Photobiol.* 70 (1):10–34. [https://doi.org/10.1562/0031-8655\(1999\)070<0010:IRACOP>2.3.CO;2](https://doi.org/10.1562/0031-8655(1999)070<0010:IRACOP>2.3.CO;2).
- D'Andrilli, J., Foreman, C.M., Marshall, A.G., McKnight, D.M., 2013. Characterization of IHSS pony Lake fulvic acid dissolved organic matter by electrospray ionization Fourier transform ion cyclotron resonance mass spectrometry and fluorescence spectroscopy. *Org. Geochem.* 65:19–28. <https://doi.org/10.1016/j.orggeochem.2013.09.013>.
- Del Panno, M.T., Morelli, I.S., Engelen, B., Berthe-Corti, L., 2005. Effect of petrochemical sludge concentrations on microbial communities during soil bioremediation. *FEMS Microbiol. Ecol.* 53 (2):305–316. <https://doi.org/10.1016/j.femsec.2005.01.014>.
- Deng, D., Lin, X., Ou, J., Wang, Z., Li, S., Deng, M., Shu, Y., 2015. Efficient chemical oxidation of high levels of soil-sorbed phenanthrene by ultrasound induced, thermally activated persulfate. *Chem. Eng. J.* 265:176–183. <https://doi.org/10.1016/j.cej.2014.12.055>.
- Fang, F., Kanan, S., Patterson, H.H., Cronan, C.S., 1998. A Spectrofluorimetric study of the binding of carbofuran, carbaryl, and aldicarb with dissolved organic matter. *Anal. Chim. Acta* 373 (2–3):139–151. [https://doi.org/10.1016/S0003-2670\(98\)00392-4](https://doi.org/10.1016/S0003-2670(98)00392-4).
- Fernández-González, A.J., Martínez-Hidalgo, P., Cobo-Díaz, J.F., Villadas, P.J., Martínez-Molina, E., Toro, N., Tringe, S.G., Fernández-López, M., 2017. The rhizosphere microbiome of burned holm-oak: potential role of the genus *Arthrobacter* in the recovery of burned soils. *Sci Rep* 7.
- Ferretto, N., Tedetti, M., Guigue, C., Mounier, S., Redon, R., Goutx, M., 2014. Identification and quantification of known polycyclic aromatic hydrocarbons and pesticides in complex mixtures using fluorescence excitation-emission matrices and parallel factor analysis. *Chemosphere* 107:344–353. <https://doi.org/10.1016/j.chemosphere.2013.12.087>.
- Festa, S., Coppotelli, B.M., Morelli, I.S., 2016a. Comparative bioaugmentation with a consortium and a single strain in a phenanthrene-contaminated soil: impact on the bacterial community and biodegradation. *Appl. Soil Ecol.* 98:8–19. <https://doi.org/10.1016/j.apsoil.2015.08.025>.
- Festa, S., Macchi, M., Cortés, F., Morelli, I.S., Coppotelli, B.M., 2016b. Monitoring the impact of bioaugmentation with a PAH-degrading strain on different soil microbiomes using pyrosequencing. *FEMS Microbiol. Ecol.* 92 (8):1–12. <https://doi.org/10.1093/femsec/fiw125>.
- Gan, S., Lau, E.V., Lau, E.V., Ng, H.K., 2009. Remediation of soils contaminated with polycyclic aromatic hydrocarbons (PAHs). *J. Hazard. Mater.* 172 (2–3):532–549. <https://doi.org/10.1016/j.jhazmat.2009.07.118>.
- Goicoechea, H.C., Yu, S., Moore, A.F.T., Campiglia, A.D., 2012. Four-way modeling of 4.2 K time-resolved excitation emission fluorescence data for the quantitation of polycyclic aromatic hydrocarbons in soil samples. *Talanta* 101:330–336. <https://doi.org/10.1016/j.talanta.2012.09.035>.
- Goldstein, A.H., 1986. Bacterial solubilization of mineral phosphates: historical perspective and future prospects. *American Journal of Alternative Agriculture* → Am. J. Altern. Agric. 1 (2):51–57. <https://doi.org/10.1017/S0889189300000088>.
- Griffiths, B.S., Philippot, L., 2013. Insights into the resistance and resilience of the soil microbial community. *FEMS Microbiol. Rev.* 37 (2):112–129. <https://doi.org/10.1111/j.1574-6976.2012.00343.x>.
- Gupta, S., Pathak, B., Fulekar, M.H., 2015. Molecular approaches for biodegradation of polycyclic aromatic hydrocarbon compounds: a review. *Rev. Environ. Sci. Biotechnol.* 14 (2):241–269. <https://doi.org/10.1007/s11157-014-9353-3>.
- Hill, M.O., 1973. Diversity and evenness: a unifying notation and its consequences. *Ecology* 54, 427–432.
- Hudson, N., Baker, A., Reynolds, D., 2007. Fluorescence analysis of dissolved organic matter in natural. Waste and polluted waters- a review. *River Res. Appl.* 23 (2007): 631–649. <https://doi.org/10.1002/rra>.
- Huesemann, M.H., Hausmann, T.S., Fortman, T.J., 2004. Does bioavailability limit biodegradation? A comparison of hydrocarbon biodegradation and desorption rates in aged soils. *Biodegradation* 15 (4):261–274. <https://doi.org/10.1023/B:BIOD.0000042996.03551.f4>.
- Jonsson, S., Persson, Y., Frankki, S., van Bavel, B., Lundstedt, S., Haglund, P., Tysklind, M., 2007. Degradation of polycyclic aromatic hydrocarbons (PAHs) in contaminated soils by Fenton's reagent: a multivariate evaluation of the importance of soil characteristics and PAH properties. *J. Hazard. Mater.* 149 (1):86–96. <https://doi.org/10.1016/j.jhazmat.2007.03.057>.
- Jost, L., 2006. Entropy and diversity. *Oikos* 113:363–375. <https://doi.org/10.1111/j.2006.0030-1299.14714.x>.
- Jouanneau, Y., Meyer, C., Duraffourg, N., 2016. Dihydroxylation of four- and five-ring aromatic hydrocarbons by the naphthalene dioxygenase from *Sphingomonas* CHY-1. *Appl. Microbiol. Biotechnol.* 100 (3):1253–1263. <https://doi.org/10.1007/s00253-015-7050-y>.
- Jung, J., Park, W., 2015. *Acinetobacter* species as model microorganisms in environmental microbiology: current state and perspectives. *Appl. Microbiol. Biotechnol.* 99 (6): 2533–2548. <https://doi.org/10.1007/s00253-015-6439-y>.
- Kandeler, E., Gerber, H., 1988. Short-term assay of soil urease activity using colorimetric determination of ammonium. *Biol. Fertil. Soils* 6 (1):68–72. <https://doi.org/10.1007/BF00257924>.
- Kulik, N., Goi, A., Trapido, M., Tuhkanen, T., 2006. Degradation of polycyclic aromatic hydrocarbons by combined chemical pre-oxidation and bioremediation in creosote contaminated soil. *J. Environ. Manag.* 78 (4):382–391. <https://doi.org/10.1016/j.jenvman.2005.05.005>.
- Lebeau, T., 2011. *Bioaugmentation for In Situ Soil Remediation: How to Ensure the Success of Such a Process*. In: Singh, A., Parmar, N., Kuhad, R.C. (Eds.), *Bioaugmentation, Biostimulation and Biocontrol, Soil Biology*. Springer-Verlag, Berlin Heidelberg, p. 129e186.
- Lee, E.J., Karoonathairiri, N., Kim, H.S., Park, J.H., Cha, C.J., Kao, C.M., Roe, J.H., 2005. A master regulator oB governs osmotic and oxidative response as well as differentiation via a network of sigma factors in *Streptomyces coelicolor*. *Mol. Microbiol.* 57 (5): 1252–1264. <https://doi.org/10.1111/j.1365-2958.2005.04761.x>.
- Lemaire, J., Laurent, F., Leyval, C., Schwartz, C., Buès, M., Simonnot, M.O., 2013a. PAH oxidation in aged and spiked soils investigated by column experiments. *Chemosphere* 91 (3):406–414. <https://doi.org/10.1016/j.chemosphere.2012.12.003>.
- Lemaire, J., Bues, M., Kabeche, T., Hanna, K., Simonnot, M.O., 2013b. Oxidant selection to treat an aged PAH contaminated soil by in situ chemical oxidation. *J. Environ. Chem. Eng.* 1 (4):1261–1268. <https://doi.org/10.1016/j.jece.2013.09.018>.
- Liang, C., Huang, C.F., Mohanty, N., RKurakalva, R.M., 2008. A rapid spectrophotometric determination of persulfate anion in ISCO. *Chemosphere* 73 (9):1540–1543. <https://doi.org/10.1016/j.chemosphere.2008.08.043>.
- Liao, J., Wang, J., Jiang, D., Wang, M.C., Huang, Y., 2015. Long-term oil contamination causes similar changes in microbial communities of two distinct soils. *Appl. Microbiol. Biotechnol.* 99 (23):10299–10310. <https://doi.org/10.1007/s00253-015-6880-y>.
- Lim, M.W., Lau, E.V., Poh, P.E., 2016. A comprehensive guide of remediation technologies for oil contaminated soil - present works and future directions. *Mar. Pollut. Bull.* 109 (1):14–45. <https://doi.org/10.1016/j.marpolbul.2016.04.023>.
- Liu, H., Bruton, T.A., Doyle, F.M., Sedlak, D.L., 2014. In situ chemical oxidation of contaminated groundwater by persulfate: decomposition by Fe(III)- and Mn(IV)-containing oxides and aquifer materials. *Environ. Sci. Technol.* 48 (17):10330–10336. <https://doi.org/10.1021/es502056d>.
- Lladó, S., Gràcia, E., Solanas, A.M., Viñas, M., 2013. Fungal and bacterial microbial community assessment during bioremediation assays in an aged creosote-polluted soil. *Soil Biol. Biochem.* 67:114–123. <https://doi.org/10.1016/j.soilbio.2013.08.010>.
- Madigan, M.T., 2005. *Anoxygenic phototrophic bacteria from extreme environments. Discoveries in Photosynthesis*. Springer, Netherlands, pp. 969–983.
- Margesin, R., Zimmerbauer, A., Schinner, F., 1999. Soil lipase activity - a useful indicator of oil biodegradation. *Biotechnol. Tech.* 13 (12):859–863. <https://doi.org/10.1023/A:1008928308695>.
- Margesin, R., Feller, G., Hämmerle, M., Stegner, U., Schinner, F., 2002. A colorimetric method for the determination of lipase activity in soil. *Biotechnol. Lett.* 24:27–33. <https://doi.org/10.1006/abio.1995.0063>.
- Matzek, L.W., Carter, K.E., 2016. Activated persulfate for organic chemical degradation: a review. *Chemosphere* 151:178–188. <https://doi.org/10.1016/j.chemosphere.2016.02.055>.
- McGenity, T.J., Folwell, B.D., McKew, B.A., Sanni, G.O., 2012. Marine crude-oil biodegradation: a central role for interspecies interactions. *Aquat. Biosys.* 8 (1):10. <https://doi.org/10.1186/2046-9063-8-10>.
- Merdy, P., Achard, R., Samaali, I., Lucas, I., 2014. Selective extraction of PAHs from a sediment with structural preservation of natural organic matter. *Chemosphere* 107, 476–479.
- Mora, V.C., Rosso, J.A., Carrillo Le Roux, G., Mártire, D.O., Gonzalez, M.C., 2009. Thermally activated peroxydisulfate in the presence of additives: a clean method for the degradation of pollutants. *Chemosphere* 75 (10):1405–1409. <https://doi.org/10.1016/j.chemosphere.2009.02.038>.
- Mora, V.C., Madoño, L., Peluffo, M., Rosso, J.A., Del Panno, M.T., Morelli, I.S., 2014. Remediation of phenanthrene-contaminated soil by simultaneous persulfate chemical oxidation and biodegradation processes. *Environ. Sci. Pollut. Res.* 21 (12):7548–7556. <https://doi.org/10.1007/s11356-014-2687-0>.
- Muyzer, G., De Waal, E.C., Uitterlinden, A.G., 1993. Profiling of complex microbial populations by denaturing gradient gel electrophoresis analysis of polymerase chain reaction-amplified genes coding for 16S rRNA. *Appl. Environ. Microbiol.* 59 (3): 695–700 (doi:0099-2240/93/030695-06\$0200/0).
- Muyzer, G., Brinkhoff, T., Nübel, U., Santegoeds, C., Schäfer, H., Wawer, C., 1998. Denaturing gradient gel electrophoresis (DGGE) in microbial ecology. *Mol. Microb. Ecol.* 3, 1–27.
- Oleszczuk, P., 2007. Investigation of potentially bioavailable and sequestered forms of polycyclic aromatic hydrocarbons during sewage sludge composting. *Chemosphere* 70 (2):288–297. <https://doi.org/10.1016/j.chemosphere.2007.06.011>.
- Oserby, I.T., 2006. ISCO technology overview: do you really understand the chemistry? *Contaminated Soils, Sediments and Water: Success and Challenges*:pp. 287–308 https://doi.org/10.1007/0-387-28324-2_19.
- Pardo, F., Rosas, J.M., Santos, A., Romero, A., 2015. Remediation of a biodiesel blend-contaminated soil with activated persulfate by different sources of iron. *Water Air Soil Pollut.* 226 (2). <https://doi.org/10.1007/s11270-014-2267-4>.
- Parks, D.H., Tyson, G.W., Hugenholtz, P., Beiko, R.G., 2014. STAMP: statistical analysis of taxonomic and functional profiles. *Bioinformatics* 30 (21):3123–3124. <https://doi.org/10.1093/bioinformatics/btu494>.
- Peluffo, M., Pardo, F., Santos, A., Romero, A., 2015. Use of different kinds of persulfate activation with iron for the remediation of a PAH-contaminated soil. *Sci. Total Environ.* 563:649–656. <https://doi.org/10.1016/j.scitotenv.2015.09.034>.

- Plaza, C., Xing, B., Fernández, J.M., Senesi, N., Polo, A., 2009. Binding of polycyclic aromatic hydrocarbons by humic acids formed during composting. *Environ. Pollut.* 157 (1): 257–263. <https://doi.org/10.1016/j.envpol.2008.07.016>.
- Ranc, B., Faure, P., Croze, V., Simonnot, M.O., 2016. Selection of oxidant doses for in situ chemical oxidation of soils contaminated by polycyclic aromatic hydrocarbons (PAHs): a review. *J. Hazard. Mater.* 312:280–297. <https://doi.org/10.1016/j.jhazmat.2016.03.068>.
- Reasoner, D.J., Geldreich, E.E., 1985. A new medium for the enumeration and subculture of bacteria from potable water. *Appl. Environ. Microbiol.* 49 (1), 1–7.
- Richardson, S.D., Lebron, B.L., Miller, C.T., Aitken, M.D., 2011. Recovery of phenanthrene-degrading bacteria after simulated in situ persulfate oxidation in contaminated soil. *Environ. Sci. Technol.* 45 (2):719–725. <https://doi.org/10.1021/es102420r>.
- Rivas, F.J., 2006. Polycyclic aromatic hydrocarbons sorbed on soils: a short review of chemical oxidation based treatments. *J. Hazard. Mater.* 138 (2):234–251. <https://doi.org/10.1016/j.jhazmat.2006.07.048>.
- Rodriguez-Diaz, M., Rodelas-Gonzales, B., Pozo-Clemente, C., Martinez-Toled, M.V., Gonzalez-Lopez, J., 2008. A review on the taxonomy and possible screening traits of plant growth promoting rhizobacteria. In: Ahmad, I., Pichtel, J., Hayat, S. (Eds.), *Plant-Bacteria Interactions: Strategies and Techniques to Promote Plant Growth*, Chap. 4. Weinheim: Wiley-VCH, pp. 55–80.
- Sayara, T., Sarà, M., Sánchez, A., 2010. Optimization and enhancement of soil bioremediation by composting using the experimental design technique. *Biodegradation* 21 (3):345–356. <https://doi.org/10.1007/s10532-009-9305-8>.
- Schloss, P.D., Westcott, S.L., Ryabin, T., Hall, J.R., Hartmann, M., Hollister, E.B., Lesniewski, R.A., Oakley, B.B., Parks, D.H., Robinson, C.J., Sahl, J.W., Stres, B., Thallinger, G.G., Van Horn, D.J., Weber, C.F., 2009. Introducing Mothur: open-source, platform-independent, community-supported software for describing and comparing microbial communities. *Appl. Environ. Microbiol.* 75 (23):7537–7541. <https://doi.org/10.1128/AEM.01541-09>.
- Seo, J.S., Keum, Y.S., Li, Q.X., 2009. Bacterial degradation of aromatic compounds. *Int. J. Environ. Res. Public Health* 6 (1):278–309. <https://doi.org/10.3390/ijerph6010278>.
- Ser, H.L., Tan, L.T.H., Palanisamy, U.D., Abd Malek, S.N., Yin, W.F., Chan, K.G., Goh, B.H., Lee, L.H., 2016. *Streptomyces* antioxidants Sp. Nov., a novel mangrove soil actinobacterium with antioxidative and neuroprotective potentials. *Front. Microbiol.* 7 (JUN):1–14. <https://doi.org/10.3389/fmicb.2016.00899>.
- Shirshova, L.T., Ghabbour, E.A., Davies, G., 2006. Spectroscopic characterization of humic acid fractions isolated from soil using different extraction procedures [J]. *Geoderma* 133 (1):204–216. <https://doi.org/10.1016/j.geoderma.2005.07.007>.
- Sirguy, C., de Souza e Silva, P.T., Schwartz, C., Simonnot, M.O., 2008. Impact of chemical oxidation on soil quality. *Chemosphere* 72 (2):282–289. <https://doi.org/10.1016/j.chemosphere.2008.01.027>.
- Sparks, D.L., 1996. *Methods of soil analysis, chemical methods*. In: USA. Madison, WI (Ed.), *Methods of Soil Analysis, Chemical Methods*.
- Stokes, J.D., Paton, G.I., Semple, K.T., 2006. Behaviour and assessment of bioavailability of organic contaminants in soil: relevance for risk assessment and remediation. *Soil Use Manag.* 21:475–486. <https://doi.org/10.1079/SUM2005347>.
- Su, Y., Chen, F., Liu, Z., 2015. Comparison of optical properties of chromophoric above or below the tree line: insights into sources. *Photochem. Photobiol. Sci.* 14 (5): 1047–1062. <https://doi.org/10.1039/c4pp00478g> (Royal Society of Chemistry).
- Sun, B., Wang, F., Jiang, Y., Li, Y., Dong, Z., Li, Z., Zhang, X.X., 2014. A long-term field experiment of soil transplantation demonstrating the role of contemporary geographic separation in shaping soil microbial community structure. *Ecol. Evol.* 4 (7): 1073–1087. <https://doi.org/10.1002/ece3.1006>.
- Sutton, N.B., van Gaans, P., Langenhoff, A.A.M., Maphosa, F., Smidt, H., Grotenhuis, T.C., Rijnaarts, H.H.M., 2013. Biodegradation of aged diesel in diverse soil matrices: impact of environmental conditions and bioavailability on microbial remediation capacity. *Biodegradation* 24 (4):487–498. <https://doi.org/10.1007/s10532-012-9605-2>.
- Sutton, N.B., Langenhoff, A.A.M., Lasso, D.H., Van Der Zaan, B., van Gaans, P., Maphosa, F., Smidt, H., Grotenhuis, T.C., Rijnaarts, H.H.M., 2014a. Recovery of microbial diversity and activity during bioremediation following chemical oxidation of diesel contaminated soils. *Appl. Microbiol. Biotechnol.* 98 (6):2751–2764. <https://doi.org/10.1007/s00253-013-5256-4>.
- Sutton, N.B., Grotenhuis, T.C., Rijnaarts, H.H.M., 2014b. Impact of organic carbon and nutrients mobilized during chemical oxidation on subsequent bioremediation of a diesel-contaminated soil. *Chemosphere* 97:64–70. <https://doi.org/10.1016/j.chemosphere.2013.11.005>.
- Sutton, N.B., Kalisz, M., Krupanek, J., Marek, J., Grotenhuis, T.C., Smidt, H., De Weert, J., Rijnaarts, H.H.M., Van Gaans, P., Keijzer, T., 2014c. Geochemical and microbiological characteristics during in situ chemical oxidation and in situ bioremediation at a diesel contaminated site. *Environ. Sci. Technol.* 48 (4):2352–2360. <https://doi.org/10.1021/es404512a>.
- Swift, R.S., 1996. *Organic matter characterization. Methods of Soil Analysis Part 3—Chemical Methods*, pp. 1011–1069 (methodssoilan3).
- Szczepaniak, Z., Czarny, J., Staninska-Pięta, J., Lisiecki, P., Zgoła-Grzeškowiak, A., Cyplik, P., Chrzanowski, Ł., Wolko, Ł., Marecik, R., Juzwa, W., Glazar, K., Piotrowska-Cyplik, A., 2016. Influence of soil contamination with PAH on microbial community dynamics and expression level of genes responsible for biodegradation of PAH and production of rhamnolipids. *Environ. Sci. Pollut. Res.* 23 (22):23043–23056. <https://doi.org/10.1007/s11356-016-7500-9>.
- Tamaki, H., Wright, C.L., Li, X., Lin, Q., Hwang, C., Wang, S., Thimmapuram, J., Kamagata, Y., Liu, W.T., 2011. Analysis of 16S rRNA amplicon sequencing options on the roche/454 next-generation titanium sequencing platform. *PLoS One* 6 (9):6–8. <https://doi.org/10.1371/journal.pone.0025263>.
- Tsibart, A.S., Gennadiev, A.N., 2013. Polycyclic aromatic hydrocarbons in soils: sources, behavior, and indication significance (a review). *Eurasian Soil Sci.* 46 (7):728–741. <https://doi.org/10.1134/S1064229313070090>.
- Tsionaki, A., Petri, B., Crimi, M.L., Mosbæk, H., Siegrist, R.L., Bjerg, P.L., 2010. In situ chemical oxidation of contaminated soil and groundwater using persulfate: a review. *Crit. Rev. Environ. Sci. Technol.* 2013 (December):37–41. <https://doi.org/10.1080/10643380802039303>.
- Usman, M., Faure, P., Hanna, K., Abdelmoula, M., Ruby, C., 2012. Application of magnetite catalyzed chemical oxidation (Fenton-like and persulfate) for the remediation of oil hydrocarbon contamination. *Fuel* 96:270–276. <https://doi.org/10.1016/j.fuel.2012.01.017>.
- Valderrama, C., Alessandri, R., Aunola, T., Cortina, J.L., Gamisans, X., Tuhkanen, T., 2009. Oxidation by Fenton's reagent combined with biological treatment applied to a creosote-contaminated soil. *J. Hazard. Mater.* 166 (2–3):594–602. <https://doi.org/10.1016/j.jhazmat.2008.11.108>.
- Vatsavai, K., Goicoechea, H.C., Campiglia, A.D., 2008. Direct quantification of monohydroxy-polycyclic aromatic hydrocarbons in synthetic urine samples via solid-phase extraction-room-temperature fluorescence excitation-emission matrix spectroscopy. *Anal. Biochem.* 376, 213–220.
- Vecchioli, G.L., Del Panno, M.T., Paineira, M.T., 1990. Use of selected autochthonous soil bacteria to enhanced degradation of hydrocarbons in soil. *Environ. Pollut.* 67: 249–258. [https://doi.org/10.1016/0269-7491\(90\)90190-N](https://doi.org/10.1016/0269-7491(90)90190-N).
- Venkataramanan, K.P., Jones, S.W., McCormick, K.P., Kunjeti, S.G., Ralston, M.T., Meyers, B.C., Papoutsakis, E.T., 2013. The clostridium small RNome that responds to stress: the paradigm and importance of toxic metabolite stress in *C. acetobutylicum*. *BMC Genomics* 14 (1), 849.
- Verchot, L.V., Borelli, T., 2005. Application of Para-Nitrophenol (pNP) enzyme assays in degraded tropical soils. *Soil Biol. Biochem.* 37 (4):625–633. <https://doi.org/10.1016/j.soilbio.2004.09.005>.
- Viñas, M., Sabaté, J., Espuny, M.J., Solanas, A.M., 2005. Bacterial community dynamics and polycyclic aromatic hydrocarbon degradation during bioremediation of heavily creosote-contaminated soil. Bacterial community dynamics and polycyclic aromatic hydrocarbon degradation during bioremediation of heavily creosote. *Appl. Environ. Microbiol.* 71 (11):7008–7018. <https://doi.org/10.1128/AEM.71.11.7008-7018.2005>.
- Westersund, J., Fernandes, L., Jones, S., Clought, H., 2006. Stimulating anaerobic reductive dechlorination following chemical oxidation treatment. *Proceedings of the Fifth International Conference on Remediation of Chlorinated and Recalcitrant Compounds*. Battelle, Monterey, p. D-56.
- Whalen, J.K., Warman, P.R., 1996. Arylsulfatase activity in soil and soil extracts using natural and artificial substrates. *Biol. Fertil. Soils* 23, 373–378.
- Wrenn, B.A., Venosa, A., 1996. Selective enumeration of aromatic and aliphatic hydrocarbon-degrading bacteria by a most probable number procedure. *J. Microbiol.* 42, 252–258.
- Yoon, J.-H., Kang, S.-J., Oh, H.W., Oh, T.-K., 2007. *Pedobacter insulae* Sp. Nov., isolated from soil. *Int. J. Syst. Evol. Microbiol.* 57 (9):1999–2003. <https://doi.org/10.1099/ijso.0.64986-0>.
- Zhu, L., Ding, W., Feng, L.J., Kong, Y., Xu, J., Xu, X.Y., 2012. Isolation of aerobic denitrifiers and characterization for their potential application in the bioremediation of oligotrophic ecosystem. *Bioresour. Technol.* 108 (1–7). <https://doi.org/10.1016/j.biortech.2011.12.033>.
- Zuber, P., 2009. Management of oxidative stress in *Bacillus*. *Annu. Rev. Microbiol.* 63, 575–597.